Communication: Towards catalytic nitric oxide reduction via oligomerization on boron doped graphene

Valentina Cantatore[a)] and Itai Panas
Department of Chemistry and Chemical Engineering, Energy & Materials, Chalmers University of Technology, Gothenburg, Sweden

We use density functional theory to describe a novel way for metal free catalytic reduction of nitric oxide NO utilizing boron doped graphene. The present study is based on the observation that boron doped graphene and O—N=N—O$^-$ act as Lewis acid-base pair allowing the graphene surface to act as a catalyst. The process implies electron assisted N=N bond formation prior to N—O dissociation. Two $N_2 + O_2$ product channels, one of which favoring N_2O formation, are envisaged as outcome of the catalytic process. Besides, we show also that the $N_2 + O_2$ formation pathways are contrasted by a side reaction that brings to $N_3O_3^-$ formation and decomposition into $N_2O + NO_2^-$. *Published by AIP Publishing.* [http://dx.doi.org/10.1063/1.4947216]
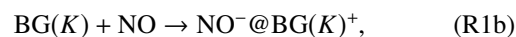
Today, the use of the remarkable electronic properties of graphene[1] to contribute new functionalities to surface coatings and composite materials is increasingly being explored. It is anticipated that with increased demand, efficient processes minimizing production prices will emerge. When considering technologies that may utilize to the fullest the particular physical and related chemical properties of a single atomic layer thick yet macroscopic compound, heterogeneous photocatalysis is among the first which come to mind.[2–4] This is owing to the ideal singular surface-to-bulk ratio, the conductivity, and the chemical variability of graphene with regard to doping as well as functionalization. The purpose of the present study is to provide a demonstrator validating this claim and do this for catalytic nitric oxide reduction. Indeed, efficient utilization of fuel in ordinary combustion engines has formation of thermal nitrogen oxides as an unwanted byproduct. One way to reduce NOx emission is to run the engine with a larger fuel/air ratio, however, the drawback is incomplete combustion of the fuel. A second approach is to employ a NOx storage/reduction (NSR) catalyst[5] which combines long periods of lean running conditions during which the NOx is trapped in an oxide, mainly barium oxide, with short fat periods during which the trapped NOx is released and reduced to N_2 by the fuel. The NOx absorption by BaO requires oxidation of the thermal nitrogen oxide,[6–10] i.e., NO, which becomes converted to NO_2 on a platinum catalyst.[11–13] Conversely, following the release of NO_2 from BaO, the reduction to N_2 takes place on a rhodium catalyst.[14] We investigate the possible utilization of functionalized boron doped graphene in circumventing the above Pt/BaO/Rh catalyst system. In doing so, the ability of boron doped graphene BG to trap NO as adsorbed $(NO)_2^-$ and $(NO)_3^-$ is exploited. These intermediate compounds are stabilized by the high electron affinity of NO oligomer anions owing to formation of robust N—N bonding.[15,16] The

required electrons would be accessed by, e.g., photocatalysis employing functional substituents directly bound to the graphene substrate achieving functionality analogous to graphene-TiO_2 composites. Recently, a reversible socket-plug Lewis acid/base functionality for boron doped graphene acting electrophile versus any incoming nucleophile was demonstrated.[17] Here, this reversible functionality is utilized in a catalytic context, where $(NO)_n^-$ act as nucleophiles. Indeed, in a series of combined experimental and theoretical studies we have explored the electron catalyzed oligomerisation and decomposition of $(NO)_n^-$, n = 2-8.[15,18,19] Here, we combine our insights of NO chemistry and Lewis acid-base socket-plug functionality of boron doped graphene towards an incoming nucleophile to explore the possible catalytic properties of the latter towards direct disproportionation of NO to $N_2 + O_2$. Thus, our study is complementary to recent NO reduction studies which utilize edge states of graphene and employ graphene as reducing agent in producing, e.g., CO_2.[20,21]

In what follows, a first scan of direct reduction pathway and bifurcation points is provided. Thus, an indirect reduction pathway involving intermediate epoxides decorated graphene is contrasted by a direct pathway. Throughout, results for single electron assisted heterogeneous oligomerization of NO molecules (Fig. 1) are compared to those employing potassium as reducing agent (Fig. 2). Enthalpy as well as Gibbs energy changes at 300 K is estimated from total energy calculations. In particular, zero-point vibration contributions are assumed to cancel. Entropy changes for adsorption/desorption of gas phase species are taken from experiment. Thus,

$$BG^- + NO \rightarrow NO^-@BG, \qquad (R1a)$$
$$\Delta H = -0.395 \text{ eV}; \ \Delta G(300 \text{ K}) = +0.261 \text{ eV}.$$
$$BG(K) + NO \rightarrow NO^-@BG(K)^+, \qquad (R1b)$$
$$\Delta H = -0.084 \text{ eV}; \ \Delta G(300 \text{ K}) = +0.571 \text{ eV},$$

followed by

[a)]Author to whom correspondence should be addressed. Electronic mail: valcan@chalmers.se
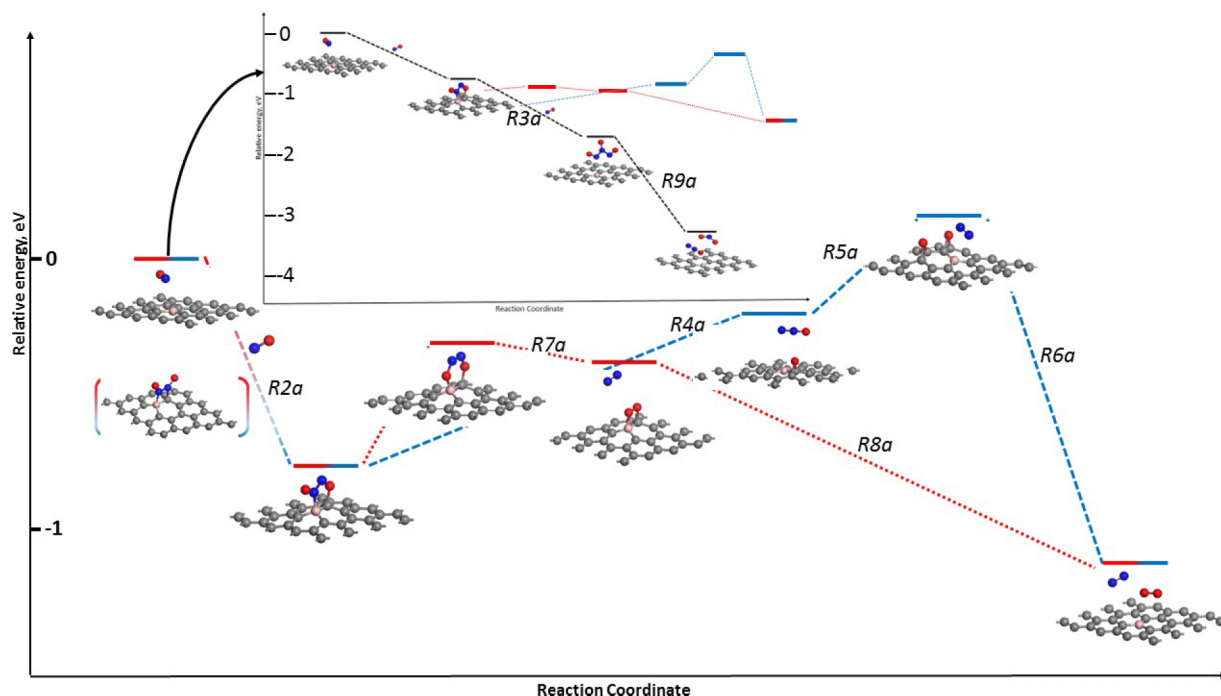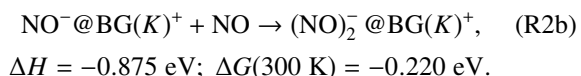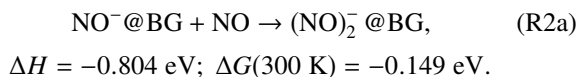
144, 151102-1

FIG. 1. Reaction paths and optimized geometry for photocatalytic NO reduction (see references to the equations in the text). Energies are referred to the first step, taken as zero. Pink: boron, blue: nitrogen, red: oxygen, grey: carbon.

$$\text{NO}^-@\text{BG} + \text{NO} \rightarrow (\text{NO})_2^-@\text{BG}, \qquad (\text{R2a})$$

$$\Delta H = -0.804 \text{ eV}; \ \Delta G(300 \text{ K}) = -0.149 \text{ eV}.$$

$$\text{NO}^-@\text{BG}(K)^+ + \text{NO} \rightarrow (\text{NO})_2^-@\text{BG}(K)^+, \qquad (\text{R2b})$$

$$\Delta H = -0.875 \text{ eV}; \ \Delta G(300 \text{ K}) = -0.220 \text{ eV}.$$

As expected, formation of $(\text{NO})_2^-$ from $2\text{NO}(g)$ is highly temperature dependent, i.e., photoelectron assisted $(\text{NO})_2^-$ formation is estimated to be barely endergonic, i.e., $\Delta G(300 \text{ K}) = +0.112 \text{ eV}$, while having a K atom act electron source results in $\Delta G(300 \text{ K}) = +0.351 \text{ eV}$. At 200 K, the two
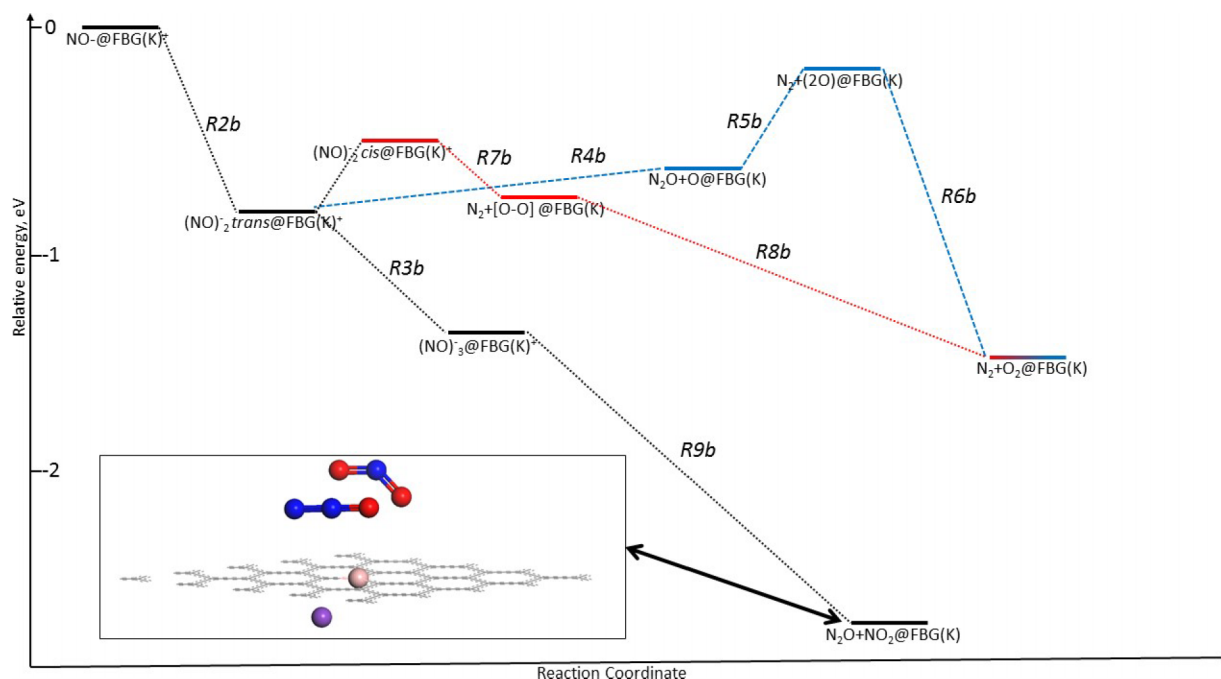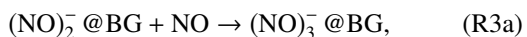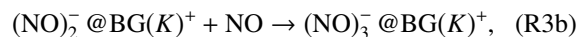

FIG. 2. Reaction paths for photocatalytic NO reduction in the presence of potassium as reducing agent. Energies are referred to the first step, taken as zero. Inset: Final structure along the N_3O_3^- + K^+ disproportionation channel to produce N_2O and NO_2 indicating proximity of potassium to the boron site. Pink: boron, purple: potassium, blue: nitrogen, red: oxygen, grey: carbon.

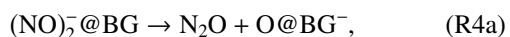reactions become spontaneous. Connection to previous work[15] is made by considering formation of the trimer

$$(NO)_2^- @BG + NO \rightarrow (NO)_3^- @BG, \qquad (R3a)$$
$$\Delta H = -0.958 \text{ eV}; \ \Delta G(300 \text{ K}) = -0.303 \text{ eV}.$$
$$(NO)_2^- @BG(K)^+ + NO \rightarrow (NO)_3^- @BG(K)^+, \quad (R3b)$$
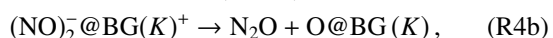$$\Delta H = -0.558 \text{ eV}; \ \Delta G(300 \text{ K}) = +0.096 \text{ eV}.$$

Again, the temperature control is emphasized in that at 200 K both ways to form the trimer become spontaneous. Finally, it is noted that the adsorption enthalpies are underestimated in that the van der Waals contribution to the adsorption was not included, rendering room temperature increased relevance.

Having established the central intermediates, characterized by formation of N=N double-bonds prior to N—O dissociation, attention is turned to essential segments of the energy landscape of the reversed NO formation reaction resulting in recovery of N_2, O_2 as well as the recovery of BG^- or $BG(K)$. One channel for utilization of BG for NO reduction employs its ability to act as an intermediate oxygen sink, i.e., forming graphene oxide to be recovered by subsequent reduction. The route which displays O_2 evolution at the tail end, involving formation of nitrous oxide N_2O intermediates is addressed,
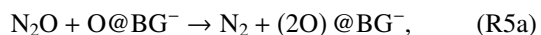
$$(NO)_2^- @BG \rightarrow N_2O + O@BG^-, \qquad (R4a)$$
$$\Delta H = 0.461 \text{ eV}; \ \Delta G(300 \text{ K}) = -0.223 \text{ eV}.$$
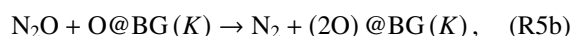$$(NO)_2^- @BG(K)^+ \rightarrow N_2O + O@BG(K), \qquad (R4b)$$
$$\Delta H = 0.191 \text{ eV}; \ \Delta G(300 \text{ K}) = -0.493 \text{ eV}.$$

While this reaction is indeed spontaneous at room temperature, complete reduction of NO into N_2 along this path requires the heterogeneous reduction of the intermediate N_2O, i.e.,

$$N_2O + O@BG^- \rightarrow N_2 + (2O)@BG^-, \qquad (R5a)$$
$$\Delta H = 0.389 \text{ eV}; \ \Delta G(300 \text{ K}) = +0.478 \text{ eV}.$$
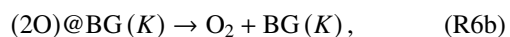$$N_2O + O@BG(K) \rightarrow N_2 + (2O)@BG(K), \quad (R5b)$$
$$\Delta H = 0.454 \text{ eV}; \ \Delta G(300 \text{ K}) = +0.543 \text{ eV}.$$

Several different strategies exist for the recovery of the catalyst. The present study offers the simple release of O_2 for reference,

$$(2O)@BG^- \rightarrow O_2 + BG^-, \qquad (R6a)$$
$$\Delta H = -1.334 \text{ eV}; \ \Delta G(300 \text{ K}) = -1.972 \text{ eV}.$$
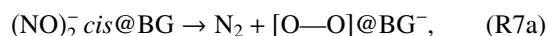$$(2O)@BG(K) \rightarrow O_2 + BG(K), \qquad (R6b)$$
$$\Delta H = -1.341 \text{ eV}; \ \Delta G(300 \text{ K}) = -1.979 \text{ eV}.$$
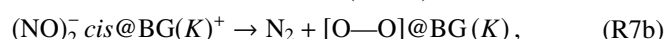
The fact that graphene oxide evolves O_2 with significant exothermicity, i.e., comprising a powerful oxidant, supports previous theoretical studies which report oxidation of NO to NO_2 by graphene oxide as one viable reaction.[22] Here we observe however that because formation of graphene oxide is in fact endothermic, both N_2 and N_2O may act as reducing agents towards graphene oxide at low temperatures, thus competing with the oxygen evolution reaction. At room temperature though, only (R5) is endergonic. The fact that the

opposite reaction is spontaneous implies that complementary strategies should be adopted to reduce the laughing gas.[23]

The second main channel at the trifurcation point offered by the $N_2O_2^-$ moiety utilizes the fact that this surface compound has three isomers comprising a four-member *cis* ring, a five-member *trans* ring, as well as a six-member *cis* ring structure. While the four-member *cis* ring structure may support direct O_2 formation, the reaction coordinate involves partial dissociation of the N=N bond to allow O—O bond formation. This is in contrast to the six-member *cis* ring structure, which offers N_2 to leave while at the same time forming an O—O peroxy bond, thus allowing for the reaction
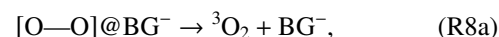
$$(NO)_2^- cis@BG \rightarrow N_2 + [O-O]@BG^-, \qquad (R7a)$$
$$\Delta H = -0.084 \text{ eV}; \ \Delta G(300 \text{ K}) = -0.68 \text{ eV}.$$
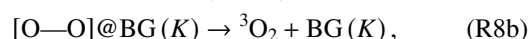$$(NO)_2^- cis@BG(K)^+ \rightarrow N_2 + [O-O]@BG(K), \qquad (R7b)$$
$$\Delta H = -0.292 \text{ eV}; \ \Delta G(300 \text{ K}) = -0.888 \text{ eV},$$

to take place. The adsorption of two oxygen atoms on adjacent graphene sites, as a four-ring peroxo moiety, has previously been suggested to offer an intermediate to the oxygen desorption where end-on superoxo transition state is described.[24] Thus, the sought final product is accessed by
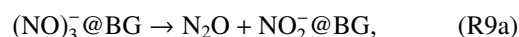
$$[O-O]@BG^- \rightarrow {}^3O_2 + BG^-, \qquad (R8a)$$
$$\Delta H = -0.750 \text{ eV}, \ \Delta G(300 \text{ K}) = -1.388 \text{ eV}.$$
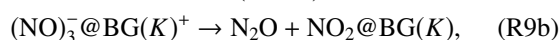$$[O-O]@BG(K) \rightarrow {}^3O_2 + BG(K), \qquad (R8b)$$
$$\Delta H = -0.737 \text{ eV}; \ \Delta G(300 \text{ K}) = -1.375 \text{ eV}.$$

It is important to note that the residual drive to form ${}^3O_2$ is sufficient to also form ${}^1O_2$. The importance of the latter O_2 desorption channel is because it is spin conserving as the peroxo intermediate also represents a singlet state. This channel would dominate on pristine graphene, however, the boron doping is understood to offer spin catalysis[25,26] rendering access to the ${}^3O_2$ ground state upon dissociation. Interestingly, it is the high entropy of the irreversible N_2O evolution channel which promotes the formation of graphene oxide, while it is the enthalpic instability of this graphene oxide which renders the direct $N_2 + O_2$ evolution channel, via the *cis* six member ring, competitive. This in turn is taken to imply preference for the latter direct reaction at low temperatures, while elevated temperatures favor the N_2O + graphene oxide channel.

A further consequence of the stability of the $N_2O_2^-$ intermediate is access to a third reaction channel involving the further oligomerization of NO. With increased complexity the number of fragmentation channels increases. Here, this is demonstrated for the binding of a third nitric oxide molecule to $N_2O_2^-(ads)$ to produce $N_3O_3^-(ads)$. This channel is essential as it bypasses both the direct $N_2 + O_2$ evolution channel and the oxidation of graphene in that N_2O and NO_2^- are formed,

$$(NO)_3^- @BG \rightarrow N_2O + NO_2^- @BG, \qquad (R9a)$$
$$\Delta H = -0.804 \text{ eV}; \ \Delta G(300 \text{ K}) = -1.448 \text{ eV}.$$
$$(NO)_3^- @BG(K)^+ \rightarrow N_2O + NO_2@BG(K), \qquad (R9b)$$
$$\Delta H = -1.342 \text{ eV}; \ \Delta G(300 \text{ K}) = -2.026 \text{ eV}.$$

With the subsequent recombination of hole-photoelectron pair, NO_2 is finally released. This competition between the $N_2O_2^-$ and $N_3O_3^-$ channels of fragmentation is understood to serve as a tool to bridge theory and experiment.

In conclusion, the direct reduction of nitric oxide including competing pathways has served to validate the possible utilization of boron doped graphene in metal-free catalysis. Energy landscapes, reflecting claimed socket-plug functionality, were provided for channels of NO decomposition into N_2, N_2O, NO_2, O_2 via the $N_2O_2^-$ and $N_3O_3^-$ intermediates, while also underscoring the sensitivity of spontaneity to temperature. Higher electron assisted polymerization of NO has been described previously offering ever higher complexity of the resulting fragments. Any selectivity among different channels, offered by boron doped graphene associated intermediates, is left for future studies. Moreover, realization of the demonstrated catalytic nitric oxide reduction understanding is presently attempted by making contact with conventional nano-particle supported heterogeneous catalysis technologies. These investigations utilize first and foremost the generic van der Waals interaction to attach boron doped graphene to the candidate substrates. Further additional stability by any Lewis base property of the support is also explored. Having said this, it is recognized that such competition for the boron sites should be carefully avoided here as these are needed to stabilize the crucial anionic nitric oxide oligomer transients.

For all the results presented in this work, a 4×4 graphene supercell (32 atoms including the boron atom) plus adsorbates was employed. All the results were obtained using the CASTEP program package[27] within the Material Studio 6.1[28] framework in conjunction with the PBE GGA functional.[29] Core electrons were described by ultrasoft pseudopotentials[30] and 380 eV cut-off energy and a $4 \times 4 \times 1$ grid for Brillouin zone sampling was used. Atomic positions were optimized with the BFGS algorithm using delocalized internal coordinates. The present study is conventional in that it assumes the existence of a well-defined Born-Oppenheimer potential energy surface (BO-PES) on which reactions occur as heat is added to the system. One implication of this assumption is that the life-times of intermediates are long as compared to the time scale of all evolving relaxations involved in their stabilizations. In reality, the time scales may be of similar orders to the extent that heterogeneous processes may involve transient dissipation of thermal energy on collision with the substrate. Such transient non-equilibrium events in turn may provide a life-time to adsorbate-substrate compounds, which do not exist on the BO-PES. It is understood that such transient inelastic processes, while not included in the present study, too are helpful in the formations of the necessary nitric oxide oligomer transients.

[1]K. S. Novoselov, A. K. Geim, S. V. Morozov, D. Jiang, Y. Zhang, S. V. Dubonos, I. V. Grigorieva, and A. A. Firsov, Science **306**(5696), 666 (2004).

[2]Q. Xiang, J. Yu, and M. Jaroniec, Chem. Soc. Rev. **41**(2), 782 (2012).

[3]Y. Zhang, Z.-R. Tang, X. Fu, and Y.-J. Xu, ACS Nano **5**(9), 7426 (2011).

[4]N. Zhang, Y. Zhang, and Y.-J. Xu, Nanoscale **4**(19), 5792 (2012).

[5]K. Yoshida, Y. Nozaki, T. Mori, Y. Bisaiji *et al.*, SAE Technical Paper No. 2014-01-2809, 2014.

[6]P. Broqvist, H. Grönbeck, E. Fridell, and I. Panas, Catal. Today **96**(1–2), 71 (2004).

[7]P. Broqvist, H. Grönbeck, E. Fridell, and I. Panas, J. Phys. Chem. B **108**(11), 3523 (2004).

[8]P. Broqvist, I. Panas, and H. Grönbeck, J. Phys. Chem. B **109**(19), 9613 (2005).

[9]P. Broqvist, I. Panas, and H. Grönbeck, J. Phys. Chem. B **109**(32), 15410 (2005).

[10]P. Broqvist, I. Panas, E. Fridell, and H. Persson, J. Phys. Chem. B **106**(1), 137 (2002).

[11]L. Castoldi, I. Nova, L. Lietti, and P. Forzatti, Catal. Today **96**(1–2), 43 (2004).

[12]L. Lietti, P. Forzatti, I. Nova, and E. Tronconi, J. Catal. **204**(1), 175 (2001).

[13]I. Nova, L. Lietti, L. Castoldi, E. Tronconi, and P. Forzatti, J. Catal. **239**(1), 244 (2006).

[14]W. S. Epling, L. E. Campbell, A. Yezerets, N. W. Currier, and J. E. Parks, Catal. Rev. **46**(2), 163 (2004).

[15]A. Snis and I. Panas, Mol. Phys. **91**(5), 951 (1997).

[16]M. A. Vincent, I. H. Hillier, and L. Salsi, Phys. Chem. Chem. Phys. **2**(4), 707 (2000).

[17]V. Cantatore and I. Panas, Carbon **104**, 40 (2016).

[18]A. Snis and I. Panas, Chem. Phys. **221**(1–2), 1 (1997).

[19]A. Snis and I. Panas, Chem. Phys. Lett. **305**(3–4), 285 (1999).

[20]A. M. Oyarzún, L. R. Radovic, and T. Kyotani, Carbon **86**, 58 (2015).

[21]A. M. Oyarzún, A. J. A. Salgado-Casanova, X. A. García-Carmona, and L. R. Radovic, Carbon **99**, 472 (2016).

[22]M. Hou, W. Cen, H. Zhang, J. Liu, H. Yin, and F. Wei, Appl. Surf. Sci. **339**, 55 (2015).

[23]A. Snis and I. Panas, Surf. Sci. **412–413**, 477 (1998).

[24]D. Yafei, N. Shuang, L. Zhenyu, and Y. Jinlong, J. Phys.: Condens. Matter **25**(40), 405301 (2013).

[25]L. Yang, S. Jiang, Y. Zhao, L. Zhu, S. Chen, X. Wang, Q. Wu, J. Ma, Y. Ma, and Z. Hu, Angew. Chem. **123**(31), 7270 (2011).

[26]T. Ikeda, M. Boero, S.-F. Huang, K. Terakura, M. Oshima, J.-i. Ozaki, and S. Miyata, J. Phys. Chem. C **114**(19), 8933 (2010).

[27]S. J. Clark, M. D. Segall, C. J. Pickard, P. J. Hasnip, M. I. J. Probert, K. Refson, and M. C. Payne, Z. Kristallogr. **220**(5/6), 567 (2005).

[28]Material Studio 6.0 Accelrys Inc. Simulation Software, 2011.

[29]J. P. Perdew, K. Burke, and M. Ernzerhof, Phys. Rev. Lett. **77**(18), 3865 (1996).

[30]D. Vanderbilt, Phys. Rev. B **41**(11), 7892 (1990).